THE BIOCLIMATE OF CHOLERA: THE CASE OF HAITI

STEPHEN TENNENBAUM, CAROLINE FREITAG, AND SVETLANA ROUDENKO

SUMMARY

Background Although cholera exhibits seasonal patterns in endemic regions, *dynamical* models describing the cholera epidemic in Haiti to date have not incorporated real-time climatic and oceanographic data in their analysis.

Methods We propose a simple model with two infective classes in order to model the cholera epidemic in Haiti. We include the impact of environmental events on the epidemic in the Artibonite and Ouest regions by introducing terms for the contact rate that vary with environmental conditions. To determine the timing and magnitude of these effects, we analyze weekly reported cholera cases versus rainfall and temperature for the Artibonite and Ouest regions. In addition, tidal influences were included in the Ouest region to account for residual variation in the data. We then fitted the models to new and total cases to obtain epidemic projections from April 2012 through February 2013.

Findings We project that by the end of February 2013, Artibonite will have seen between 122 and 126 thousand cholera cases, and Ouest will have seen 250 to 258 thousand cholera cases. We found lag times between precipitation events and new cases that vary seasonably, ranging from 5 to 11 weeks in Artibonite, and $5 \cdot 7$ to $8 \cdot 5$ in Ouest. In addition, it appears that, in the Quest region, tidal influences play a significant role in the dynamics of the disease.

Interpretation Intervention efforts have apparently reduced reproductive number in both regions, however persistent outbreaks of cases continue. This seems to imply that the bay and rivers have become repositories for cholera even without large outflows of human waste and that many local populations will continue to be at risk for a long time to come. Knowledge of environmental events in conjunction with the lag times may help prepare more focused and timely interventions and conserve resources.

Funding None.

INTRODUCTION

On January 12, 2010, a $7 \cdot 0$ magnitude earthquake struck near Haiti's capital, Port-au-Prince.[1] The poorest nation in the Western Hemisphere, the earthquake shattered Haiti's already weak infrastructure.[1] Thousands of Haitians were killed and even more were forced to flee to resettlement camps.[1]

In October 2010, the first case of cholera was reported in Haiti. A later UN investigation revealed the specific strain of *V. cholerae* came from South Asia.[2] The UN investigation and epidemiological literature suggest that the epidemic began outside of a UN peacekeeper camp near Mirebalais in the Centre department, along the Artibonite River.[2,3] As *V. cholerae* is a waterborne pathogen, the Artibonite River is the ostensible route through which the disease spread throughout Haiti's ten administrative regions, called departments.[4]

Anecdotal news reports describe the dismal situation for thousands of Haitians that still remain displaced months after the earthquake. Sewage of millions of people flow through open ditches. Human waste from septic pits and latrines is dumped into the canals, and after it rains, ends up in the sea. Those living close to the water use over-the-sea toilets, and next to these outhouses, fishing boats unload and sell the fish from plastic buckets...[5]

Haiti's two most populous regions, Ouest and Artibonite, were also the two regions hardest hit by the epidemic. Cases in Ouest and Artibonite account for 60% of the total burden of cholera in Haiti.[6] For this reason, we chose to focus our analyses on the Ouest and Artibonite regions. By April 7, 2012, cholera had affected $5 \cdot 7\%$ of the total population* in Ouest and $6 \cdot 9\%$ of the population in Artibonite.[6]

*Note: population data for Haiti is from 2009[4] , one year before the earthquake.

Four mathematical models describing the cholera outbreak in Haiti were published in early 2011.[7–10] The first three models proposed a variation on the SIWR model proposed by Codeço in 2001.[11] The SIWR model explains cholera transmission through susceptibles' contact with a water reservoir, rather than susceptibles' contact with infectious individuals. The models proposed by Tuite, et al.[8] and Bertuzzo, et al.[9] both incorporated a "gravity" term to study the interaction among regions. The model proposed by Andrews and Basu[7] accounted for a bacterial "hyperinfectivity" stage, following research by Hartley, et al. in 2006 showing that *V. cholerae* initially has a higher infectivity before it decays to a lower infective rate in the aquatic reservoir. The fourth model by Chaoa, et al.[10] was an agent based approach designed to look at various vaccination strategies.

In addition, all these models assessed the impact of potential intervention strategies, including vaccination. Bertuzzo found that a vaccination campaign aiming to vaccinate 150,000 people after January 1, 2011 would have little effect, in part because of the late timing and in part because of the large proportion of *asymptomatic* individuals who would need to get vaccinated.[9] Both the models proposed by Tuite, et al.[8] and Andrews and Basu[7] suggest that vaccination campaigns would have modest effect. In March 2012, Partners in Health began vaccinating 100,000 individuals with Shanchol, a two-dose cholera vaccine.[12] The size of the campaign is limited by the size of the global stockpile of Shanchol.[12] The vaccination campaign is targeted at 50,000 individuals living in the slums of Port-au-Prince, where population density is thought to increase the rate of cholera exposure, and at 50,000 individuals living in the Artibonite River valley, where the epidemic began.[12] Chao et al.[10] showed that a targeted vaccination strategy would have the best results for this limited supply of vaccine, and by vaccinating 30% of the population the cases could be reduced by as much as 55%.

In 2001, Codeço proposed introducing an oscillating term to model seasonal variability.[11] However, none of the four Haiti-specific models accounted for seasonality. Haiti experienced flooding in June 2011, October 2011, and March 2012.[13] As cholera has reached an endemic state in Haiti, an analysis of cholera's seasonality as it relates to Haiti's rainy season is pertinent. Moreover, mathematical models should incorporate seasonality in order to more accurately predict the course of the epidemic and to simulate the effects of potential interventions. In April 2012 Rinaldo et al.[14] reexamined the above four models (including their own[9]) and concluded that, among other factors, seasonal rainfall patterns were necessary to account for resurgences in the epidemic. They use long-term monthly averages to augment the bacterial growth term of contaminated water-bodies.

In this paper we use more detailed and current rainfall, temperature, and tidal records to model cholera in the Artibonite and Ouest regions. After showing the connection to previous models, we forego the bacterial compartment in favor of an *a posteriori* approach using climatic data directly to estimate infection rates. This has the advantage of more tractable temporal estimates without the need for elaborate, spatial, social and watershed networks. This paper is also the first, that we know of, that uses tidal variation in a model of cholera dynamics.

METHODS

Data. For Ouest and Artibonite, we investigated the correlations between reported cholera cases and rainfall, temperature, and in the case of Ouest, tidal range. We wanted to determine a) if such correlations exist, and b) the time delay between environmental conditions and recorded cholera outbreaks.

The source of the epidemic data was *the Haitian Ministry of Public Health and Population* and compiled by *the Pan American Health Organization*.[4,6] The data sets available, which we used for this study, consist of cumulative cholera cases, and new cholera cases. New cholera cases are calculated based on the difference between the latest report and the previous one. Cholera case definition also includes suspected cholera cases and deaths in addition to confirmed cases and deaths. As such, data posted on the web site are periodically updated with minor corrections. For instance, as of this writing, data reported after March 4, 2012 for the Ouest region are provisional. Cases are reported on weekly basis with the reporting week beginning on Sunday.

Reported hospitalized cases and hospitalized deaths are probably more accurate, but for the purposes of this study, less useful, since we want to track the progress of the epidemic, and increases in *access* to treatment biases the data. New case estimates for the first few weeks of the epidemic are unavailable. Total cases (TC) for the first 4 weeks was obtained by regressing, for the following 8 weeks (14-Nov-10 through 2-Jan-11), the reported total cases against hospitalized cases (HC). For the Ouest region $TC_O = 2 \cdot 2HC_O \ \left(R^2 = 0 \cdot 99\right)$, and for the Artibonite region $TC_A = 2 \cdot 59HC_A + 497 \ \left(R^2 = 1 \cdot 00\right)$.

Rainfall, temperature and tide data were compared to the pattern of new cholera cases reported each week. The rainfall data comes from NASA[15] , using centrally located points in each region as our datum point, given by (latitude,

longitude). For Artibonite our datum point is $(19{\cdot}125, -72{\cdot}625)$ and for Ouest, it is $(18{\cdot}625, -72{\cdot}375)$.[15] NASA updated its processing of the data during the course of this project from TRMM_3B42_daily.006 to TRMM_3B42_daily.007. Although our initial investigation used the version 6 material, all figures and parameter estimates given in this paper are using version 7. Precipitation estimates are a combination of remote sensing and ground verified information reported with a spatial resolution of $0{\cdot}25 \times 0{\cdot}25$ degrees and a temporal resolution of 1 day, further details are available on the web site.[15]

Temperature data is mean daily air temperature at Port-au-Prince, and is reported by the Weather Underground.[16] Although we had daily numbers for Temperature we chose to extract the annual cycle and use that in simulations. This has the advantage of allowing us to extrapolate temperature for model projections.

Tide data is for Port-au-Prince Bay (StationId: TEC4709).[17] These numbers are predictions from NOAA's tide model for this location and are not direct measurements. NOAA's web site allows you to download tide numbers for any date starting from 2010 and extending through 2014.

The initial modeling was done by comparing data sets in the frequency domain for new cases and rainfall in order to find any suggestions of matching periodicity and/or time-lags. Code was then written in Berkeley Madonna to simulate the dynamical system, and try various manipulations of the environmental data in order to match predictions to data*. Rainfall data was available only to week of 26-Feb-2012 (week 71) because of the lag between the timing of rainfall events and what had been processed at the time we accessed it.[15]

Model. Our preliminary conceptual model was based on previously published models describing the cholera epidemic in Haiti.[7–9] We model the Ouest and Artibonite regions separately to capture varying regional dynamics (see Figure 1).

The preliminary model is a variation on the SIWR model, which assumes that cholera is spread through *susceptibles'* (S) contact with contaminated water, food or fomites. This model uses the amount of water consumed as a proxy for all possible modes of transmission, and the concentration of bacteria in the water consumed is B (see[18] with a base model[11]). The infection rate, α, is modified by a dose-response expression $\frac{B}{K+B}$, where K is the concentration of bacteria in consumed water to cause 50% chance of infection.[11] An infectious individual may either be *symptomatic* (I) or *asymptomatic* (A).[19] The probability ρ of asymptomatic infection is $0{\cdot}79$.[19,20] Symptomatic and asymptomatic individuals contribute to the bacterial reservoir at a rate ξ_I and ξ_A, respectively.[7] W is the effective size of the environmental water repository at risk of being consumed. Both *symptomatic* and *asymptomatic* individuals move to the recovered group R at a rate γ. *Symptomatic* individuals die from cholera at a rate μ (dead are denoted by D). The bacterial reservoir concentration B grows at a rate proportional to the number of infectious individuals, characterized by the shedding rates (ξ_I and ξ_A) divided by W, the size of the regional water reservoir. Bacteria in the reservoir die at the rate μ_B.

We obtain the following dynamics of Haiti's population as described by the original system of ordinary differential equations (see Figure 1): $N = S + A + I + R + D$, where N is the initial population of the region.

Original system Reduced system

$$\left\{\begin{array}{l} \frac{dS}{dt} = -\alpha S \frac{B}{K+B} \\ \frac{dA}{dt} = \rho\alpha S \frac{B}{K+B} - \gamma A \\ \frac{dI}{dt} = (1-\rho)\alpha S \frac{B}{K+B} - (\gamma+\mu) I \\ \frac{dR}{dt} = \gamma(A+I) \\ \frac{dB}{dt} = \frac{\xi_I}{W} I + \frac{\xi_A}{W} A - \mu_B B \end{array}\right\} \implies \left\{\begin{array}{l} \frac{dS}{dt} = -\beta(t)\, S \\ \frac{dA}{dt} = \rho\beta(t)\, S - \gamma A \\ \frac{dI}{dt} = (1-\rho)\beta(t)\, S - (\gamma+\mu) I \\ \frac{dR}{dt} = \gamma(A+I) \end{array}\right\}$$

There are a number of difficulties with this preliminary model in the context of the situation in Haiti, particularly, the bacteria compartment. The first of which is that the water reservoir is ultimately much larger than the amount actually consumed and is essentially unmeasurable. Another is that the death rate of the bacteria is ostensibly the free living death rate, a full and proper model would require an extensive ecosystem model that incorporate *V. cholerae* in the guts of copepods, cysts in the sediments and so on. However, since the transmission of bacteria is regulated by environmental conditions we will combine the maximum infection rate α with the dose-response expression into a single effective infection rate: $\beta(t) = \alpha \frac{B(t)}{K+B(t)}$. The parameter $\beta(t)$ will then be estimated by fitting the number cases predicted by the model to the data, thus eliminating the problem of estimating all parameters associated with the

*When we discuss the output of our model, will use the term "prediction" to indicate the numbers generated during the calibration phase of the model and "projection" to indicate the extrapolation of the model past cases used for the calibration.

bacterial compartment as well as K (the 50% ID). We then have the reduced system of the first four equations above with $\beta(t)$ substituted as described. All other parameters are discussed below and values are given in Table 1 and Table 2.

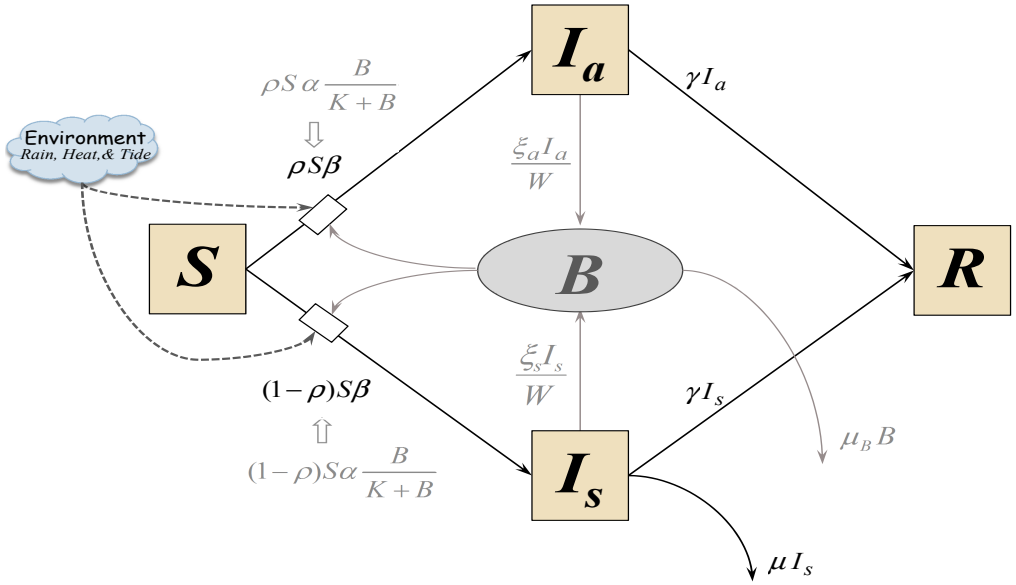

FIGURE 1. A compartmental model describing the movement of individuals from susceptible to infectious to recovered, with two infectious classes *symptomatic* and *asymptomatic*, and interaction with a bacterial reservoir. The greyed elements are in the original system and compose the bacterial sub-system that is replaced with the time-variant formula for β in the reduced system. See equation 1 and "Environmental equations" section for details on the environmental relationships.

This paper evaluates *the reduced system* separately for two regions, Artibonite and Ouest, in order to capture the varying dynamics in each region.

Model with Environmental Effects. In order to incorporate environmental effects we modified the model proposed by Codeço in 2001.[11] We assume that significant rain events will cause flooding, which will increase direct contact the bacteria via contaminated water, or indirectly via soils, vegetation, and disease bearing insects, etc. that have been contaminated or consumed cholera bacteria. We also assume that temperature plays a dual role by increasing the infection rate and decreasing the lag time between rainfall events and disease outbreaks.

Additionally, in the Ouest region there are commercial areas, tent-cities and slums that have raw waste directly discharging to Port-au-Prince Bay, or to the bay via rivers (e.g. Froide, Momance, and Grise), and numerous open sewage canals. We hypothesis that there may be additional disease generated when large tidal ranges stir up contaminated sediments or cause blooms of plankton in these coastal waters. Again the chain of infection may be complex and include direct contact with water, insects, or consumption of contaminated seafood, etc.

Therefore, we modify the contact rate β such that

$$\beta(t) = \alpha_p H(t)\, P(t-\tau_p, \theta_p) + \alpha_m M(t-\tau_m, \theta_m)\,, \tag{1}$$

where P is a moving average of the amount of daily rainfall, and M is a moving average of the maximum semi-diurnal tidal range, H is a heat index based on mean air temperature, τ_p, is the lag time for precipitation (which is itself affected by temperature), τ_m is the lag time for tides, $\theta_p, \&\theta_m$ are the averaging periods, and $\alpha_p, \&\alpha_m$ are proportionality constants.

We also included an expression for improvement of conditions over time, either through reducing the effective susceptibles, or reduction in the infection rate, or both. These factors would be due to increased access to clean water, increased personal hygiene, decreased contamination of the environment, vaccination, and rapid treatment of

new cases, or any other means of removing risk. We assume the total infection rate (βS) is reduced by an exponential decreasing factor $v(t) = e^{-rt} + (1 - e^{-rt})v_0$, where r is the rate of improvement in conditions and $1 - v_0$ is the maximum amount of improvement possible in the short term (v_0 can be considered the persistent fraction of risk remaining in a region). The final total infection rate is then $v\beta S$.

Model calibration. All modeling and calibration was done in Berkeley Madonna. When possible we used reasonable ranges for each parameter as established by previously published research (see Table 2). Since our model contains many fitted parameters, we attempted to minimize the plausible range for each parameter in order to obtain a more accurate fit. Parameter values not obtained from the literature were adjusted in an iterative fashion to narrow their initial ranges, fitting by eye predicted number of new cases to the reported number of new cases. The Berkeley Madonna curve fitting algorithm was then used to minimize the root mean square difference between model predictions of number of cumulative cases and reported cases. See Section 4.1 for a discussion of fitting the environmental terms.

RESULTS

Parameters from literature. The following table displays parameter values for each region obtained from published or online sources.

Parameter	Artibonite	Ouest	Units or calculation	References
ρ	$0{\cdot}79$	$0{\cdot}79$	fraction becoming asymptomatic	[19,21]
γ	$1{\cdot}4$	$1{\cdot}4$	fraction recovered per week	[7,9,11]
N_0	1,571,020	3,664,620	–	[4]
S_0	1,534,338	3,663,699	$N - (A_0 + I_0 + R_0 + D_0)$	
I_0	7,653	193	regression on early hospitalized cases	[6]
A_0	28,790	726	$\frac{\rho}{1-\rho} I_0$	
R_0	0	0	–	
D_0	239	2	–	[6]
t_0	17-Oct.-2010	17-Oct.-2010	290^{th} day of the year	[6]

Environmental equations.

Artibonite. Bioclimatic influences on infection rate are a product of precipitation rate and an heat index. Daily precipitation $p(t)$[15] is averaged over an interval θ_p so the running average precipitation rate is $\frac{1}{\theta_p} \sum_{j=0}^{\theta_p} p(t - \tau_p + j)$, where τ_p is the delay in precipitation's affect on infection rate (see below). The effect of precipitation is assumed to saturate at some level P_{sat} so that

$$P(t - \tau_p, \theta_p) = \min \left\{ \frac{1}{\theta_p} \sum_{j=0}^{\theta_p} p(t - \tau_p + j), P_{\text{sat}} \right\}.$$

For the delay we used a simple sine function to model a mean temperature index throughout the year. The mean air temperature index given by

$$T_{air}(t) = \sin\left(\frac{2\pi(7t + 187)}{365{\cdot}25}\right), \quad \text{where } t \text{ is in weeks from 17-Oct.-2010}^{[16]}.$$

This is then used to create a delay functions that varies from a minimum of τ_{p_lo} during summer and τ_{p_hi} during winter

$$\tau_p = ((\tau_{p\_hi} + \tau_{p\_lo}) - (\tau_{p\_hi} - \tau_{p\_lo}) T_{air}(t))/2.$$

In other words, infections result faster in the summer than in the winter months.

In addition, there is a direct influence of temperature on the infection rate. This heat index is given by

$$H(t) = 1 + kT_{air}(t).$$

Finally, the infection rate is given by

$$\beta(t) = \alpha_p H(t) P(t - \tau_p, \theta_p).$$

Note that since the maximum value of T_{air} is 1 and the maximum value of P is P_{sat}, then the maximum infection rate is $\beta_{\max} = \alpha_p(1 + k) P_{\text{sat}}$.

Ouest. For the Ouest region we use the same formulation as in Artibonite, however, we found that tidal *range* appeared to significantly affect infection rates as well. The maximum tidal range each day (there are two) $m\,(t)$[17] is averaged over an interval θ_m so the running average precipitation rate is

$$M(t-\tau_m,\theta_m)=\frac{1}{\theta_m}\sum_{j=0}^{\theta_m} m\,(t-\tau_m+j)\,,$$

where τ_m is the delay in the tide's affect on infection rate. Here, τ_m is fixed, the effect of temperature (water or air) on lengthening or shortening the response in infection rate was not found to be sufficient to warrant adding another function and additional parameters. Thus, the overall infection rate for Ouest is

$$\beta\,(t)=\alpha_p H(t)\,P(t-\tau_p,\theta_p)+\alpha_m M(t-\tau_m,\theta_m)\,.$$

Again, the maximum value of T_{air} is 1 and the maximum value of P is P_{sat}, and the maximum value of the averaged tidal range is $\max\limits_{all\ t}\{M\,(t)\}$ so that the maximum infection rate is $\beta_{\max}=\alpha_p\,(1+k)\,P_{\text{sat}}+a_m\max\limits_{all\ t}\{M\,(t)\}$.

Parameter Fitting. The following table displays parameter values for each region obtained through curve-fitting to cumulative reported cases. An explanation for curve-fitting was given in Section 3.2.

parameter	Artibonite	Ouest	units	description
θ_p	$4{\cdot}61$	$1{\cdot}96$	weeks	averaging window for precip.
τ_{p_lo}	$0{\cdot}4019$	$3{\cdot}8$	weeks	minimum delay for precip. effects
τ_{p_hi}	$7{\cdot}1805$	$6{\cdot}5$	weeks	maximum delay for precip. effects
P_{sat}	$29{\cdot}76$	$52{\cdot}106$	mm rain [daily]	saturation level of precip. effects
k	$0{\cdot}5198$	$0{\cdot}5812$	$^{\circ}\text{C}^{-1}$	temp.-precip. interaction level
α_p	$6{\cdot}8416\times10^{-3}$	$1{\cdot}0197\times10^{-3}$	$(\text{mm}\times\text{week})^{-1}$	infection rate per mm rain
θ_m	–	1	weeks	averaging window for tidal range
τ_m	–	$1{\cdot}96$	weeks	delay for tidal range effects
α_m	–	$2{\cdot}9685\times10^{-4}$	$(\text{meters}\times\text{week})^{-1}$	infection rate per meter tide range
r	$0{\cdot}06044$	$0{\cdot}02438$	week^{-1}	decrease in susceptibles per week
v_0	$0{\cdot}05$	$0{\cdot}05$	fraction	persistant fraction of pop. at risk

Lag times. The total delays in response to precipitation and tides are the sum of the averaging window and the delay function. For precipitation the minimum and maximum delays for Artibonite are $5\cdot0$ and $11\cdot8$ weeks, and for Ouest they are $5\cdot7$ and $8\cdot5$ weeks, respectively. The shorter delays are very similar in the two regions during the warmer months but during the cooler months the response time in Artibonite is 3 weeks longer. These long delays are similar in magnitude to delays reported from a study of Cholera in Zanzibar, East Africa (8 weeks fixed delay),[22]and the shorter delays (4 weeks) to those in Bangladesh.[23] For Ouest estimated delay from response to changes from tidal range was about 3 weeks. But since influence of tidal range has not been quantitatively reported elsewhere in the literature, we have nothing to compare this number to.

Although, rainfall data was available only to week of 26-Feb-2012 (week 71), we run the simulations for another month, until 1-Apr-2012 (1st day of week 76), just short of the minimum time lag between precipitation events and new cases.

Simulations and Projections. The following Figures 2 and 3 show the model predictions compared to observations for cumulative number of cases.

Epidemic projections for Artibonite. We project that by the end of February 2013, Artibonite will have seen between 122 and 126 thousand cholera cases. This is an increase of between 11 and 15 thousand cases from June 2012. Assuming 1/3 of all cholera cases are reported to the hospital[7] , Artibonite will potentially see 4 to 5 thousand hospitalized cases in the next 8 months.

Ouest. We project that by the end of February 2013, Ouest will have seen 250 to 258 thousand cholera cases. This is an increase of 26 to 34 thousand cases from June 2012. Again assuming 1/3 of all cholera cases are reported to the hospital[7] , Ouest will see 8 to 10 thousand more cases between now and February 2013.

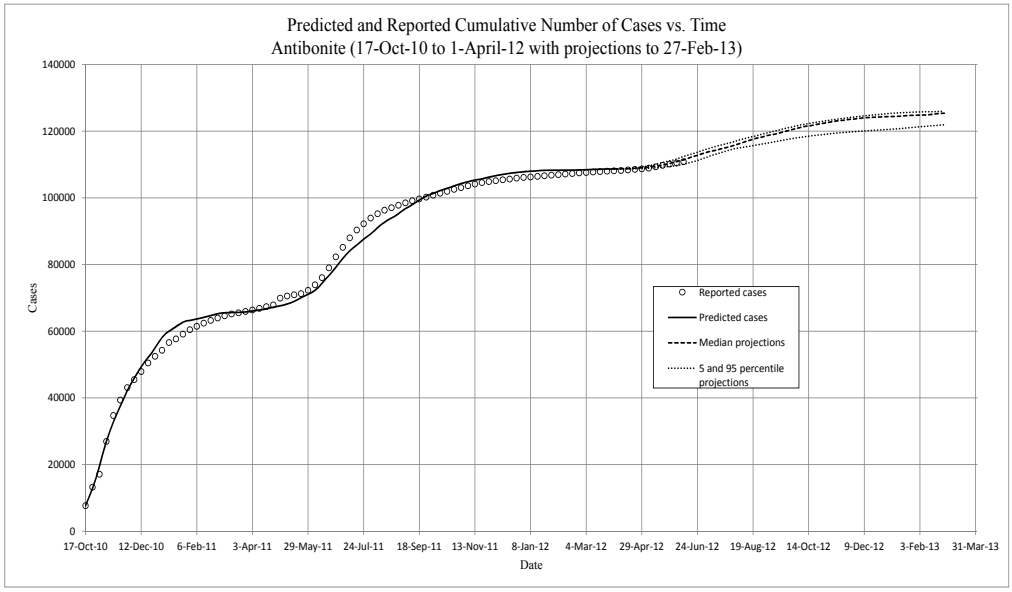

FIGURE 2. Artibonite. The predicted cumulative number of *symptomatic* individuals, against total reported cases to 1-Apr-2012. Projections from then to end of February are based on runs using prior 13 years of precipitation data.

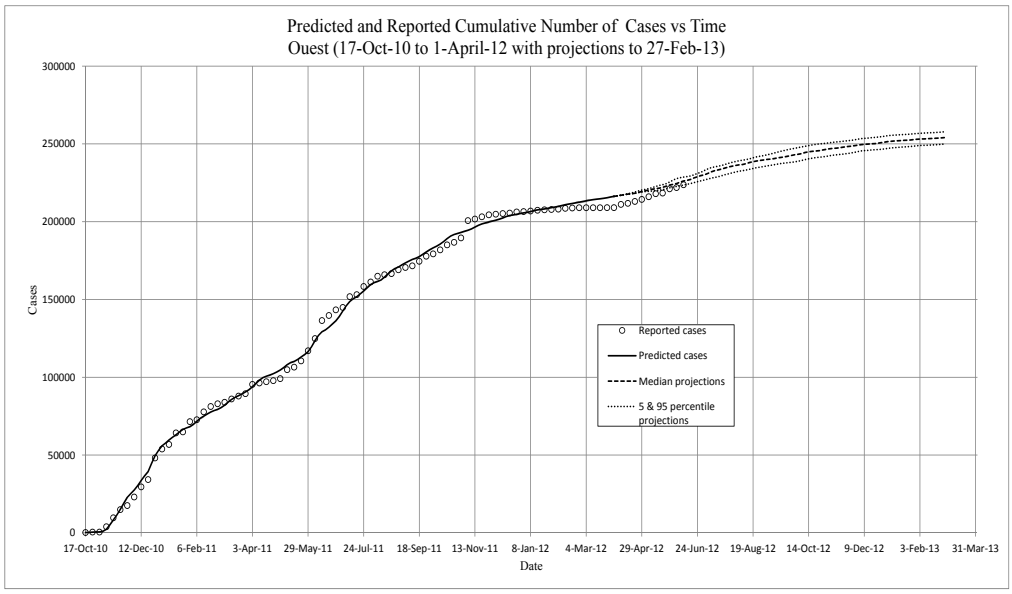

FIGURE 3. Ouest. The predicted cumulative number of *symptomatic* individuals, against total reported cases to 1-Apr-2012. Projections from then to end of February are based on runs using prior 13 years of precipitation data. Note that for the Ouest region, the model begins at the *fourth week*. We assume that the low initial numbers in the first three weeks are a result of immigration of cases from the Artibonite region. The model therefore uses data for the first four weeks – assumed immigration numbers for the first three weeks and the initialization of the model from data for the fourth week.

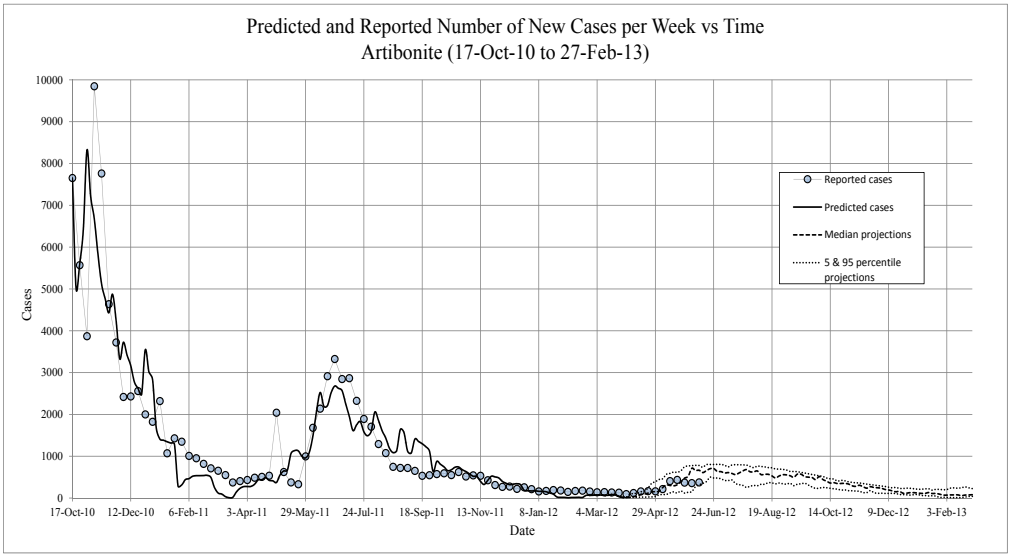

FIGURE 4. Artibonite. The new *symptomatic* individuals, vs. time. Circles - observed; solid line - model prediction; Dashed lines - 5, 50, and 95 percentiles for model projections based on past 13 years precipitation records.

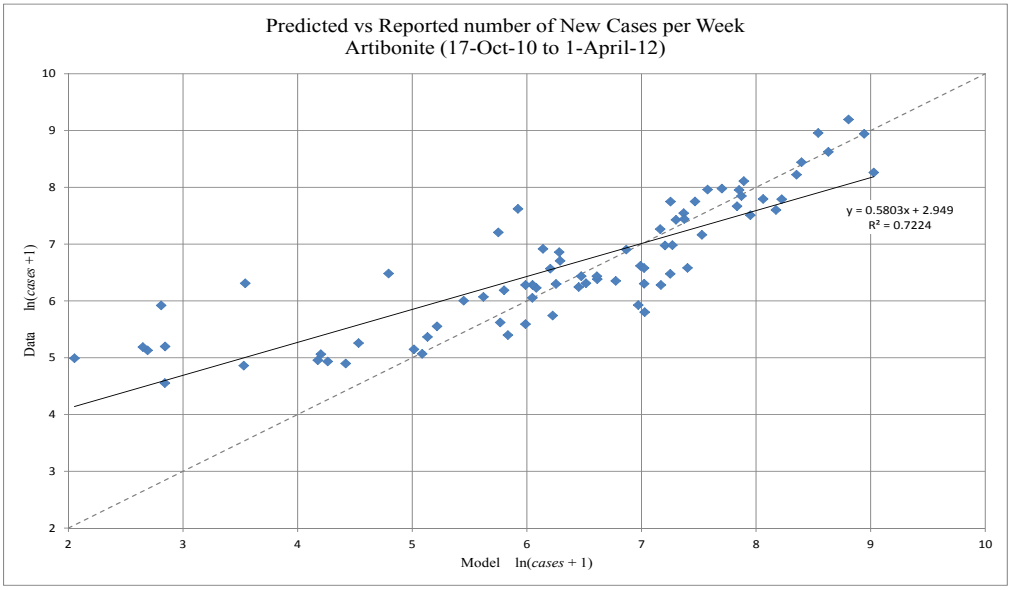

FIGURE 5. Artibonite. The predicted new *symptomatic* individuals, against weekly reported cases to 1-Apr-2012 (log-log plot). A regression line matching the main diagonal (45°) dashed line would show a perfect fit, the discrepancy is due in part to fitting on the cumulative numbers.

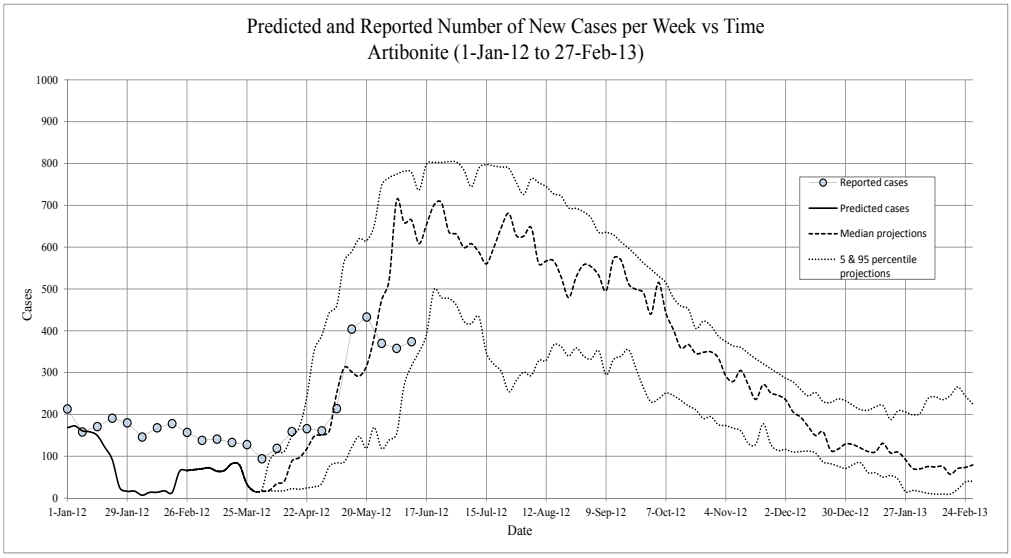

FIGURE 6. Artibonite. The projected new *symptomatic* individuals, vs. time. Circles - observed; solid line - model prediction; Dashed lines - 5, 50, and 95 percentiles for model projections based on past 13 years precipitation records.

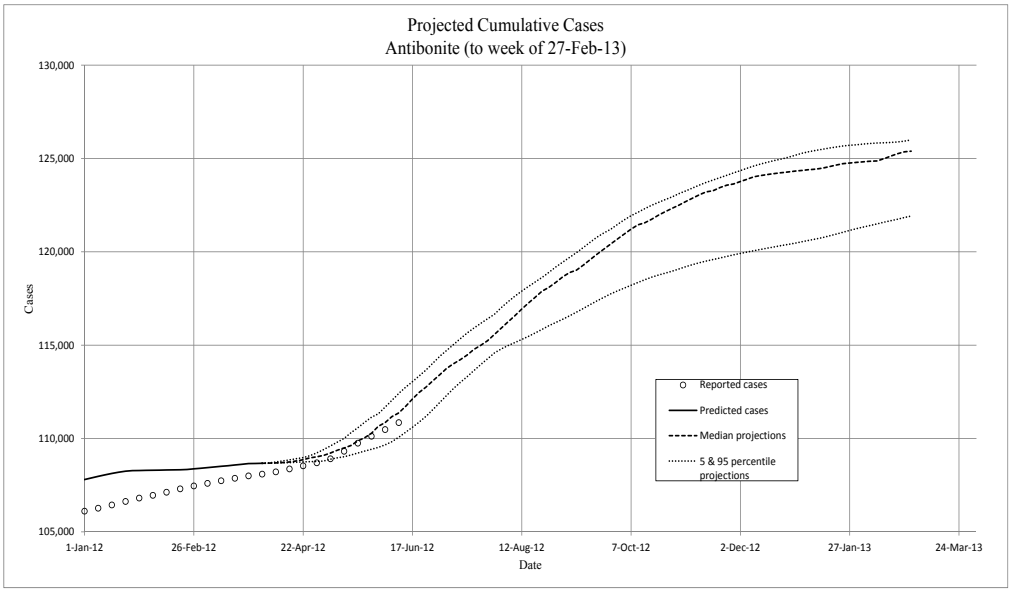

FIGURE 7. Artibonite. The projected total *symptomatic* individuals, vs. time. Circles - observed; solid line - model prediction; Dashed lines - 5, 50, and 95 percentiles for model projections based on past 13 years precipitation records.

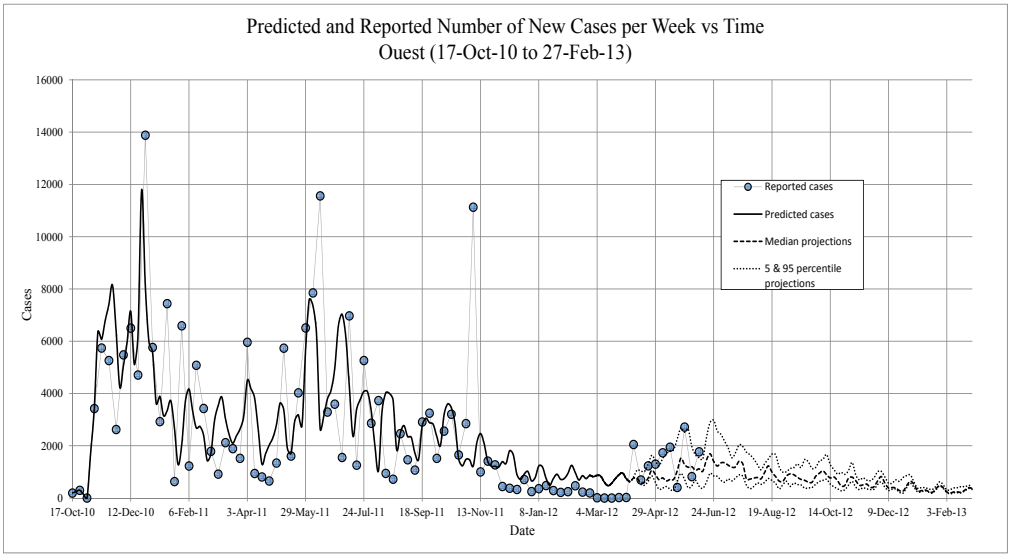

FIGURE 8. Ouest. The new *symptomatic* individuals, vs. time. Circles - observed; solid line - model prediction; Dashed lines - 5, 50, and 95 percentiles for model projections based on past 13 years precipitation records.

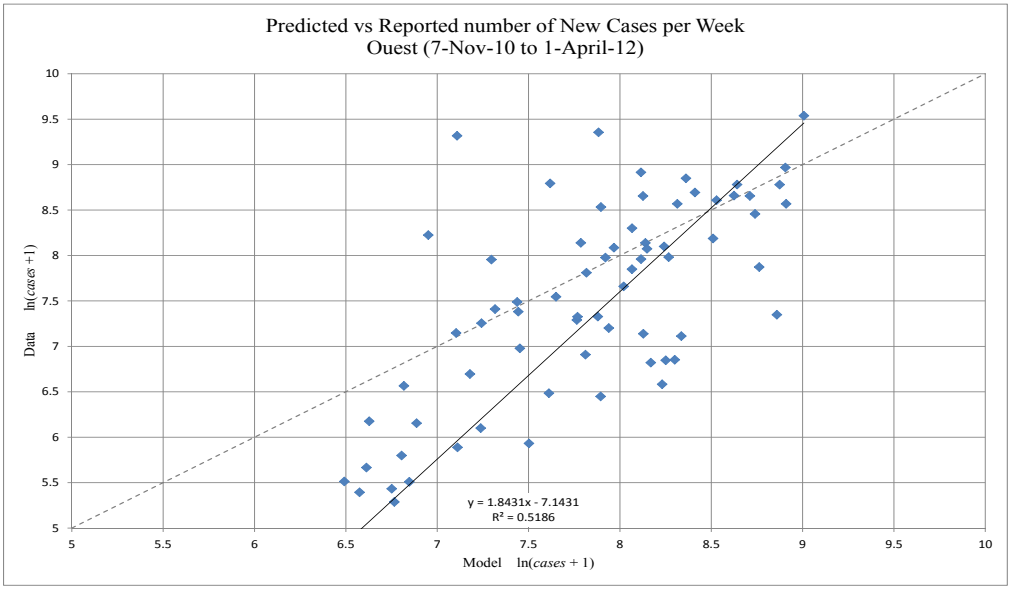

FIGURE 9. Ouest. The predicted new *symptomatic* individuals, against weekly reported cases to 1-Apr-2012 (log-log plot). A regression line matching the 45° line would show a perfect fit, the discrepancy is due in part to fitting on the cumulative numbers.

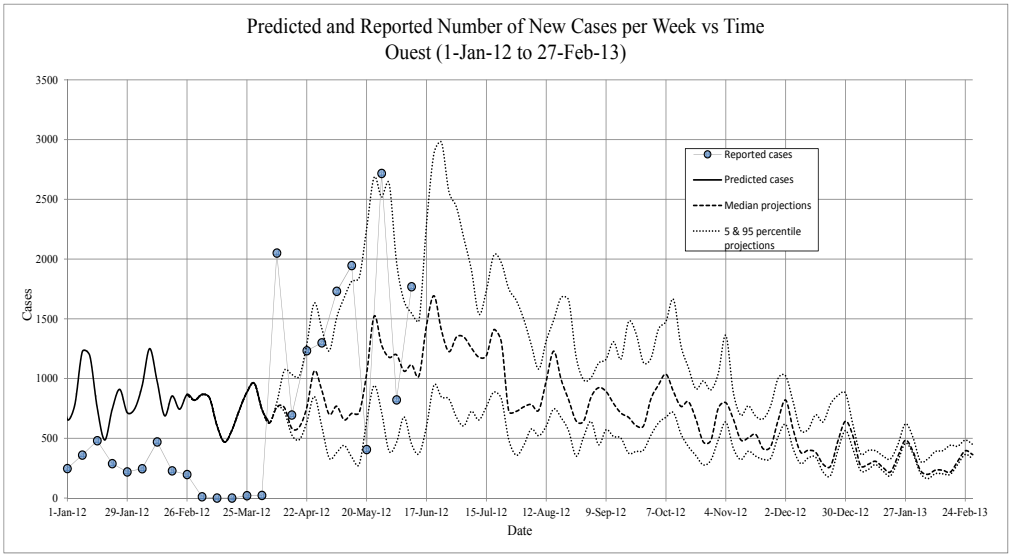

FIGURE 10. Ouest. The projected new *symptomatic* individuals, vs. time. Circles - observed; solid line - model prediction; Dashed lines - 5, 50, and 95 percentiles for model projections based on past 13 years precipitation records.

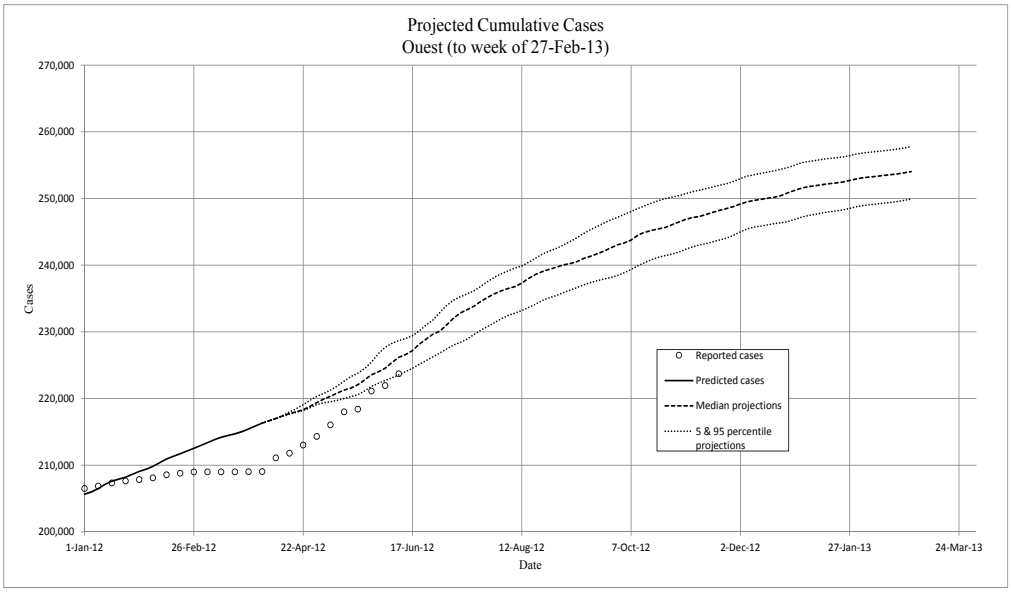

FIGURE 11. Ouest. The projected total *symptomatic* individuals, vs. time. Circles - observed; solid line - model prediction; Dashed lines - 5, 50, and 95 percentiles for model projections based on past 13 years precipitation records.

Reproductive Number $\mathcal{R}$. For the system given in section four we can write the rate of change of total number of infected individuals, both symptomatic and asymptomatic as

$$\begin{aligned}\frac{d}{dt}(I+A) &= (1-\rho)S\alpha\frac{B}{K+B} - (\gamma+\mu_c)I_s + \rho\alpha S\frac{B}{K+B} - \gamma I_a \\ &= \alpha S\frac{B}{K+B} - \left((\gamma+\mu_c)I_s + \gamma I_a\right).\end{aligned}$$

We calculate the reproductive number at any particular time as the ratio of growth terms to clearance terms, that is

$$\mathcal{R} = \alpha\frac{B}{K+B}\frac{S}{((\gamma+\mu_c)I_s+\gamma I_a)}.$$

Substituting $\beta = \alpha\frac{B}{K+B}$, we have

$$\mathcal{R} = \frac{\beta S}{((\gamma+\mu_c)I_s+\gamma I_a)}.$$

For Artibonite, we found $\mathcal{R} > 1$ about $7{\cdot}9\%$ of the time with an average value of $0{\cdot}66$. For Ouest, we found $\mathcal{R} > 1$ about $25{\cdot}2\%$ of the time with the average value of $0{\cdot}86$. Artibonite started out higher than Ouest though $2{\cdot}34$ vs. $2{\cdot}16$. We graphed the monthly moving average $\mathcal{R}$ for the Artibonite and Ouest Departments and included minimum, maximum and median projected values (Figures 12 and 13). Except for extremely wet years in Ouest the projected

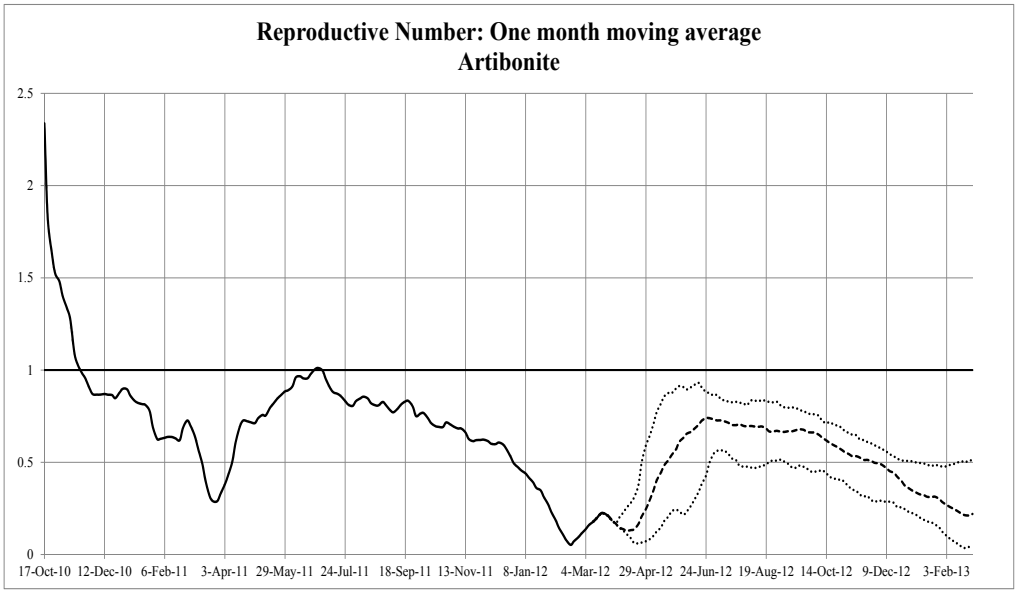

FIGURE 12. Artibonite. The monthly running average reproductive numbers. Solid line - model prediction; Dashed lines - minimum, median, and maximum for model projections based on past 13 years precipitation records. (For the 1st month averaging was done only over the length of the model run up to that point.)

reproductive numbers for both areas fall below and stay below 1 for the entire simulation. Thus, with these trends continuing persistence of the disease will depend on the bacteria surviving as cysts in sediments or as a symbiont of crustaceans in the river and bay waters, and cycling within smaller localized at risk human populations.

DISCUSSION

Use of environmental data to model the dynamics of cholera in Haiti has been hampered by the lack of historical records. We use NASA satellite data to address this problem. This study shows that with environmental data of sufficient detail and quality, projections of disease progression can be made with sufficient lead time to prepare for

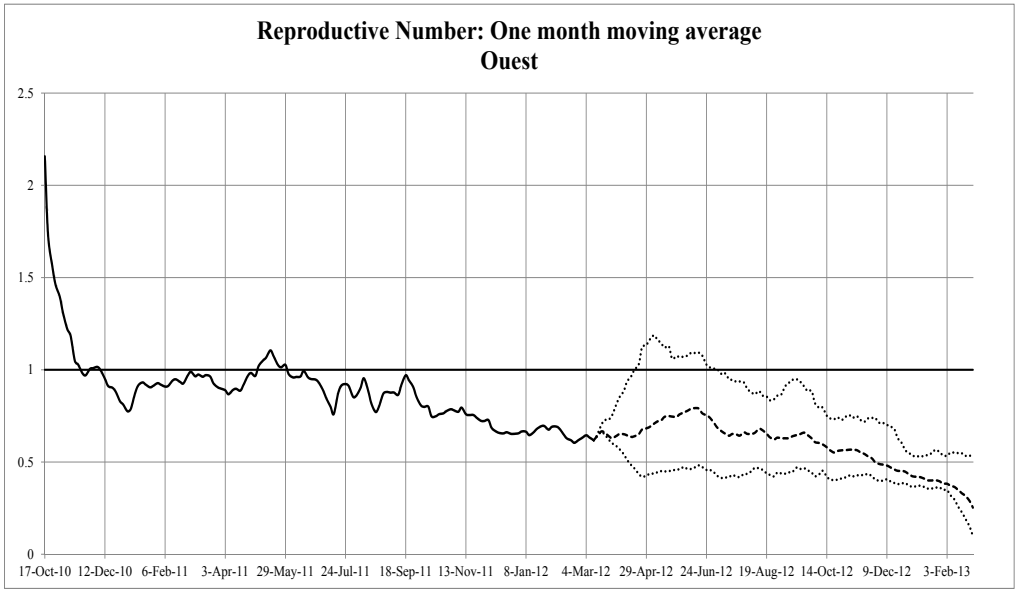

FIGURE 13. Ouest. The monthly running average reproductive numbers. Solid line - model prediction; Dashed lines - minimum, median, and maximum for model projections based on past 13 years precipitation records. (For the 1st month averaging was done only over the length of the model run up to that point.)

outbreaks. The lag times of over five weeks means that if even rudimentary but reliable meteorological and coastal records are kept, preparations and resources can be more focused. The gathering of basic weather information is simple and inexpensive and should be made standard procedure when any agency takes part in interventions, particularly when the environmental component of the epidemiology is so well established.

In addition we explored the hypothesis that, at least in the Quest region, tidal influences play a significant role in the dynamics of the disease. It appeared that tidal range rather than the height of the tide itself had the strongest influence. Some connection to tidal influences should be expected where large populations are in close contact with bays and estuaries and humans are consuming local seafood.[23,24]

We also affirmed the longer time lags (8 - 10 weeks) found in previous studies from Africa[22] and shorter ones (4 weeks) in Bangladesh.[23]

We used a system of differential equations to model the disease dynamics, however, the relationships at the core of this system were *simple* enough that once one knows what relationships to look for, the data exploration could be done in a spreadsheet.

The decline of the reproductive number in both regions with less and less episodes of $\mathcal{R}$ exceeding 1 means that there is a possibility for eradicating this disease from Haiti in a reasonable period of time if proper measures are taken and focused on the persistent populations that remain at risk. These declining numbers are for the overall population and belie the fact that many local populations are still without basic hygienic facilities. This was reflected in the model by arbitrarily setting a level v_0 to 5% of the original number of susceptible. This value matches the approximate 5% of the population that still remain displaced after the 2010 earthquake.[25]

On top of predicting when and how many cholera cases will rise with Haiti's climate and tides, any modeling to predict the effectiveness of interventions (such as vaccination) should consider these patterns. Considering that cholera may be maintained in the environment outside the human chain of infection is essential to planing effective prophylaxes and interventions.

Authors' contributions. All three authors developed the model and conceptual framework, CF and ST did most of literature search and data collection, CF wrote the first draft of the report, ST and SR drafted the final version of the report.

Conflicts of interest. We declare that we have no conflict of interest.

Research in context.

Systematic review. We reviewed the literature dealing with cholera, modeling, and climatic conditions (rainfall, precipitation, & tides) in Haiti at the beginning of this study and again at the end. We did multi-database searches in the Biology, Medicine, and Health fields and found four modeling papers[7–10] of which the first three used variations of a basic system of differential equations proposed in 2001 by Codeço.[11] At that time, none of these models took environmental conditions directly into account. Two other papers[14,26] have since appeared that do take precipitation into account in cholera. The first[26] is a spatiotemporal Markov chain model using seasonal rainfall which was outside our purview. The second[14] deals specifically with Haiti and was done by the same group that produced one of the earlier papers.[9] Here they looked at the reliability of these earlier studies, and they found that although these models do well in capturing the early dynamics of the epidemic, they fail to track latter recurrences forced by seasonal patterns.[14] As a follow up, Rinaldo et al.[14] add a precipitation forcing function to their original model along with other modifications such as the river network and population mobility. These modifications produce a better fit to the observed pattern of case and predict recurring large outbreaks tracking the projected precipitation patterns.

Other papers dealing with bio-climate were a study of Cholera in Zanzibar, East Africa that demonstrated 8 weeks fixed delay[22] between rainfall and cholera outbreaks, and another paper in Bangladesh[23] that have a somewhat shorter delay (4 weeks). Both these studies use a statistical approach with seasonal data. Both also made note of the potential influence of ocean environmental factors, and the Reyburn et al. paper included sea surface height and sea surface temperature in their analysis but failed to find any significant relationship.[22] In a third paper Koelle et al. (2005)[27] model very long time periods, more than a year, in Bangladesh. This model also uses seasonal precipitation and models changes in the susceptible fraction of the population due to demographics and loss of immunity.

Interpretation. Although much progress has been made in the past two years in modeling the Haitian cholera epidemic, only one model, so far, has accounted for seasonal variation due to precipitation, and none have examined temperature or tidal influences. Our paper shows that with basic climatic and tidal records and a relatively unsophisticated modeling procedure, not only can these factors be accounted for but also the time lags between climatic events and outbreaks can be identified. This approach looks at specific climatic events on the scale of a week rather than just seasonal patterns, and is useful in anticipating sudden rises in new cases.

We use daily tidal range as a predictive factor for cholera epidemics for the first time in a modeling paper, and we use real time daily precipitation estimates. These provide a level of detail that can help focus the location and timing of intervention and public hygiene efforts.

REFERENCES

[1] World Health Organization. WHO|Haiti.; 2012. Accessed 28 April 2012. http://www.who.int/hac/crises/hti/en/.

[2] Cravioto A, Lanata CF, Lantagne DS, Nair GB. Final Report of the Independent Panel of Experts on the Cholera Outbreak in Haiti. United Nations; 2011. Retrieved from http://www.un.org/News/dh/infocus/haiti/UN-cholera-report-final.pdf.

[3] Piarroux R, Barrais R, Faucher B, Haus R, Piarroux M, Gaudart J, et al. Understanding the Cholera Epidemic, Haiti. Emerg Infect Dis. 2011 Jul;17(7):1161–1168.

[4] Ministère de la Santé Publique et de la Population. Daily reports of MSPP on the evolution of cholera in Haiti. Republique d'Haiti; 2012. Retrieved from http://www.mspp.gouv.ht/site/index.php?option=com_content&view=article&id=120&Itemid=1.

[5] Knox R. Shots: NPR's Health Blog. Port-Au-Prince: A City Of Millions, With No Sewer System.; 2012. Accessed 2 May 2012. http://www.npr.org/blogs/health/2012/04/13/150501695/port-au-prince-a-city-of-millions-with-no-sewer-system?ps=sh_sthdl.

[6] Pan American Health Organization. Interactive Atlas of the Cholera Outbreak in La Hispaniola, 2010-2012.; 2012. Accessed 3 March 2012. http://new.paho.org/hq/images/Atlas_IHR/CholeraHispaniola/atlas.html.

[7] Andrews JR, Basu S. Transmission dynamics and control of cholera in Haiti: an epidemic model. Lancet. 2011;377:1248–1255.

[8] Tuite AR, Tien J, Eisenberg M, Earn DJ, Ma J, Fisman DN. Cholera Epidemic in Haiti, 2010: Using a Transmission Model to Explain Spatial Spread of Disease and Identify Optimal Control Interventions. Annals of Internal Medicine. 2011 May;154(9):593–601.

[9] Bertuzzo E, Mari L, Righetto L, Gatto M, Casagrandi R, Blokesch M, et al. Prediction of the spatial evolution and effects of control measures for the unfolding Haiti cholera outbreak. Geophysical Research Letters. 2011;38:L06403.

[10] Chao DL, Halloran ME, Longini IM Jr. Vaccination strategies for epidemic cholera in Haiti with implications for the developing world. Proceedings of the National Academy of Sciences. 2011 Apr;108(17):70817085.

[11] Codeço CT. Endemic and epidemic dynamics of cholera: the role of the aquatic reservoir. BMC Infectious Diseases. 2001;1:1–14. Available from: http://www.biomedcentral.com/1471-2334/1/1.

[12] Knox R. Shots: NPR's Health Blog. Vaccination Against Cholera Finally Begins in Haiti.; 2012. Accessed 2 May 2012. http://www.npr.org/blogs/health/2012/04/12/150493770/vaccination-against-cholera-finally-begins-in-haiti?ps=sh_sthdl.

[13] United Nations. Haiti|ReliefWeb.; 2012. http://reliefweb.int/country/hti.

[14] Rinaldo A, Bertuzzo E, Mari L, Righetto L, Blokesch M, Gatto M, et al. Reassessment of the 20102011 Haiti cholera outbreak and rainfall-driven multiseason projections. Proceedings of the National Academy of Sciences. 2012 Apr;109(17):66026607.

[15] NASA. NASA Earth Data. Daily TRMM and Other Satellites Precipitation Product (3B42 V7 derived) (TRMM_3B42_daily).; 2012. Accessed June 2012. http://mirador.gsfc.nasa.gov/cgi-bin/mirador/ [data files].

[16] The Weather Underground. Mean temperature (and other) weather history for Port-Au-Prince, Haiti.; 2012. Accessed 11 June 2012. http://www.wunderground.com/history/airport/MTPP/2012/1/1/CustomHistory.html.

[17] NOAA. NOAA Tides & Currents Website: Tide Predictions - Application.; 2012. Accessed 25 June 2012. http://tidesandcurrents.noaa.gov/noaatidepredictions/NOAATidesFacade.jsp?Stationid=TEC4709.

[18] Tien JH, Earn DJD. Multiple transmission pathways and disease dynamics in a waterborne pathogen model. Bulletin of Mathematical Biology. 2010;72:1506–1533.

[19] Neilan RLM, Schaefer E, Gaff H, Fister KR, Lenhart S. Modeling optimal intervention strategies for cholera. Bulletin of Mathematical Biology. 2010;72:2004–2018.

[20] Hartley DM, Morris JG Jr, Smith DL. Hyperinfectivity: A critical element in the ability of *V. cholerae* to cause epidemics? PLoS Med. 2006;3:e7.

[21] Kaper JB, Morris JG Jr, Levine MM. Cholera. Clinical Microbiology Reviews. 1995;8(1):48–86.

[22] Reyburn R, Kim DR, Emch A, Khatib A, von Seidlein L, Ali M. Climate Variability and the Outbreaks of Cholera in Zanzibar, East Africa: A Time Series Analysis. The American Journal of Tropical Medicine and Hygiene. 2011;84(6):862–869.

[23] de Magny GC, Murtugudde R, Sapiano MRP, Nizam A, Brown CW, Busalacchi AJ, et al. Environmental signatures associated with cholera epidemics. Proceedings of the National Academy of Sciences. 2008;105(46):17676–17681.

[24] Huq A, Small EB, West PA, Huq MI, Rahman R, Colwell RR. Ecological Relantionships Between *Vibrio cholerae* and Planktonic Crustacean Copepods. Applied and Environmental Microbiology. 1983;45(1):275–283.

[25] CERF (Office for the Coordination of Humanitarian Affairs - United Nations). CERF gives $8 million to support humanitarian activities in Haiti.; 2012. Accessed 10 July 2012. http://ochaonline.un.org/CERFaroundtheWorld/Haiti2012/tabid/7810/language/en-US/Default.aspx.

[26] Reiner RC Jr, King AA, Emch M, Yunus M, Faruque ASG, Pascual M. Highly localized sensitivity to climate forcing drives endemic cholera in a megacity. Proceedings of the National Academy of Sciences. 2012 Feb;109(6):20332036.

[27] Koelle K, Rodó X, Pascual M, Yunus M, Mostafa G. Refractory periods and climate forcing in cholera dynamics. Nature. 2005 Aug;436(7051):696–700.

THE GEORGE WASHINGTON UNIVERSITY, WASHINGTON DC 20052
E-mail address: set1@gwu.edu

THE GEORGE WASHINGTON UNIVERSITY, WASHINGTON DC 20052
E-mail address: calliefreitag@gmail.com

THE GEORGE WASHINGTON UNIVERSITY, WASHINGTON DC 20052
E-mail address: roudenko@gwu.edu